A new more consistent Reynolds model for piezoviscous hydrodynamic lubrication problems in line contact devices ☆

G. Bayada[a], B. Cid[b], G. García[b], C. Vázquez[c,*]

[a]ICJ UMR CNRS 5208, INSA de Lyon (France)
[b]Departamento de Matemática Aplicada II, E.E. Telecomunicación
Campus Marcosende, Universidade de Vigo, 36310 – Vigo (Spain)
[c]Departamento de Matemáticas, Universidade da Coruña
Campus Elviña s/n, 15071 – A Coruña (Spain)

Abstract

Hydrodynamic lubrication problems in piezoviscous regime are usually modeled by the classical Reynolds equation combined with a suitable law for the pressure dependence of viscosity. By taking into account the pressure–viscosity dependence in the Stokes equation and to derive the Reynolds equation in the thin film limit, a new model has been proposed by Rajagopal & Szeri. However, these authors consider some additional simplifications. In the present work, avoiding these simplifications and starting from a Stokes equation with pressure dependence of viscosity through Barus law, a new Reynolds model for line contact lubrication problems is deduced, in which the cavitation phenomenon is also taken into account. Thus, the new complete model consists of a nonlinear free boundary problem associated to the proposed new Reynolds equation.

Moreover, the classical model, the one proposed by Rajagopal & Szeri and the here proposed one are simulated through the development of some numerical algorithms involving finite elements method, projected relaxation techniques, duality type numerical strategies and fixed point iteration techniques. Finally, several numerical tests are performed to carry out a comparative analysis among the different models.

Keywords: Hydrodynamic lubrication, piezoviscous regime, Reynolds equation, cavitation phenomenon, free boundary

☆This paper has been partially funded by MEC (Project MTM2010–21135–C02).

*Corresponding author

Email addresses: Guy.Bayada@insa-lyon.fr (G. Bayada), bego@dma.uvigo.es (B. Cid), guille@dma.uvigo.es (G. García), carlosv@udc.es (C. Vázquez)

1. Introduction

In thin film lubrication problems the assumption that the viscosity of the lubricant remains constant, and therefore independent of pressure, results to be reasonable in low pressure regimes. However, when the lubricant is subjected to high pressures a strong dependence of viscosity on pressure arises, thus leading to the so called piezoviscous lubrication regimes. In the mechanical and mathematical literature concerning the models for piezoviscous hydrodynamic thin film lubrication problems, different classical devices have been considered, such as journal–bearings, rolling–bearings or rolling–ball–bearings (see [18], for example). In all of these situations, the behavior of the lubricant pressure in the thin film setting has been classically modeled by the Reynolds equation, in which the pressure dependence of viscosity is usually introduced *a posteriori* by some expression. In this procedure, the thin film limit from Stokes equation to Reynolds one is obtained regardless of the pressure–viscosity dependence, as in the case of constant viscosity (isoviscous regime). We note that in the constant viscosity case, the heuristic statement of incompressible Reynolds equation from Stokes model is obtained in [16] while the more rigorous one based on asymptotic developments is proved in [2].

In the piezoviscous case, one of the most classical expressions relating pressure and viscosity is given by the Barus law

$$\mu = \mu_0 \ \mathrm{e}^{\alpha\, p}, \tag{1}$$

where μ, μ_0, p and α denote the viscosity, the zero pressure viscosity, the pressure and the piezoviscosity coefficient, respectively. Classically in the lubrication literature, the expression (1) is plugged into Reynolds equation to model piezoviscous regimes. The resulting nonlinear Reynolds equation is then used inside more complex models that additionally consider presence of cavitation or elastohydrodynamic phenomena. In these more complex settings, this way of including piezoviscous regimes has given rise to several mathematical analysis results that state the existence and the uniqueness of solution, as well as to the design of suitable numerical methods to approximate the corresponding solutions, for which there are no analytical expressions (see, for example, [19, 11, 12, 4, 13]).

Barus law has been also used to model pressure dependence of viscosity in the original Stokes equation in [1] arguing also that Reynolds equation is only valid when the shear stress is much smaller than the reciprocal of the pressure–viscosity coefficient, while later on in [17] a corrected Reynolds equation is obtained from Navier–Stokes ones with pressure dependence of viscosity and in [14] a simpler derivation is obtained.

More recently, by assuming that the viscosity depends on pressure in Stokes equation according to Barus law, in [15] a more careful derivation of the limit Reynolds equation is carried out. The authors find additional terms to those ones appearing in the classical Reynolds equations used for elastohydrodynamic computations. Furthermore, they evaluate the consequences of these additional terms in the hydrodynamic regimes leading to high enough pressure values. This

derivation starts from the assumptions that stress tensor in the incompressible fluid includes the possibility that constraint forces could influence the work and is linear in the symmetric part of the velocity gradient tensor. Thus, unlike the Navier–Stokes equation for incompressible fluids which involves a explicit relation between both tensors and a constant viscosity, in this departure model an implicit relation holds and pressure dependence of viscosity is considered. More precisely, the departure model in the case of a steady two dimensional plane flow is given by the following equations:

$$-\frac{\partial p}{\partial x}+\mu(p)\Delta u+2\mu'(p)\frac{\partial u}{\partial x}\frac{\partial p}{\partial x}+\mu'(p)\left(\frac{\partial u}{\partial y}+\frac{\partial v}{\partial x}\right)\frac{\partial p}{\partial y}=\rho\left[u\frac{\partial u}{\partial x}+v\frac{\partial u}{\partial y}\right] \quad (2)$$

$$-\frac{\partial p}{\partial y}+\mu(p)\Delta v+\mu'(p)\left(\frac{\partial u}{\partial y}+\frac{\partial v}{\partial x}\right)\frac{\partial p}{\partial x}+2\mu'(p)\frac{\partial v}{\partial y}\frac{\partial p}{\partial y}=\rho\left[u\frac{\partial v}{\partial x}+v\frac{\partial v}{\partial y}\right] \quad (3)$$

$$\frac{\partial u}{\partial x}+\frac{\partial v}{\partial y}=0, \quad (4)$$

where x and y denote the spatial coordinates, (u, v) represents the velocity field and ρ denotes the fluid density. Note that the viscosity depends on pressure. After some simplifying assumptions detailed in [15], including that $\partial p/\partial y = 0$, equations (2)-(3) are reduced to

$$\frac{dp}{dx}=\mu\frac{\partial^2 u}{\partial y^2}+2\frac{d\mu}{dp}\frac{\partial u}{\partial x}\frac{dp}{dx}\,. \quad (5)$$

Next, by integrating (5) twice across the film and taking into account the boundary conditions for the horizontal velocity we can get an expression for $u(x, y)$. Finally, by replacing this expression in (4) and integrating again across the film for a vertical velocity v vanishing at both surfaces, the following modified Reynolds equation is obtained:

$$\frac{d}{dx}\left[\left(\frac{h^3}{\mu}-12\,\alpha\int_0^h y(h-y)\,\frac{\partial u}{\partial x}\,dy\right)\frac{dp}{dx}\right]=6\,s\,\frac{dh}{dx}, \quad (6)$$

jointly with the Barus law (1). Here h, (u, v) and $(s, 0)$ denote the gap between surfaces, the velocity field in the thin film and the given velocity of the lower sliding surface, assuming that the upper surface is fixed. Furthermore, by using the simplification

$$\frac{\partial u}{\partial x}\approx\frac{du_{av}}{dx}, \quad (7)$$

where u_{av} is an average velocity, the flow rate

$$Q=h(x)\,u_{av}(x) \quad (8)$$

is introduced in [15] to deduce the following modified Reynolds equation

$$\frac{d}{dx}\left[\left(\frac{h^3}{\mu}+\alpha\,Q\,\frac{dh^2}{dx}\right)\frac{dp}{dx}\right]=6\,s\,\frac{dh}{dx}\,. \quad (9)$$

Next, for the case of the hydrodynamic and elastohydrodynamic lubrication of a long cylinder rolling on a plane, in [15] the effect of the extra term appearing in the modified equation with respect to the classical one is numerically investigated. The chosen device parameters imply that high pressures appear, so that their computed values and those ones of the corresponding viscosities allow to illustrate the existence of differences between both models, mainly consisting in higher values for the case of modified equation.

In the present paper, we avoid the use of some simplifications considered in [15] and propose an original methodology to deduce a family of models that take into account the pressure dependence of viscosity, by solving the problem defined by equations (6), (4) and (1). More precisely, a fixed point iteration produces different models, the complexity of which ones increases with iterations. The present work focuses on the model produced by the first iteration of the algorithm, in which additional terms appear with respect to the more classical piezoviscous model, noting that for particular values of certain parameters both the isoviscous and the classical piezoviscous models can be recovered. Additionally, we model the consideration of cavitation phenomenon by means of a complementarity formulation (also known as Reynolds cavitation model). It is wellknown that this cavitation model can be formulated in terms of a variational inequality. Moreover, we propose two different numerical methods to solve the new model: the first one based on the second order differential equation problem and the second one on a first order equation. By using these numerical methods, the hydrodynamic behavior of the lubricant film in the presence of sufficiently high pressures for the three piezoviscous models can be compared.

The paper is organized as follows. In section 2 the here proposed model is presented. Section 3 describes the cavitation model here considered and the scaling. The reduction to an initial value problem associated to first order ordinary differential equation is stated in section 4. In Section 5 the numerical methods are described. Numerical results are presented in Section 6. Finally, in Section 7 some considerations about conclusions and future work are summarized.

2. An alternative Reynolds equation for piezoviscous lubrication

As indicated in the introduction, in the present work we mainly propose a more rigorous way to obtain a piezoviscous model avoiding the simplification (7) that has been considered to state the modified Reynolds equation (9). The proposed methodology to deduce a new family of models is based on a fixed point technique to solve the coupled system defined by equations (6), (4) and (1).

For this purpose, we start by considering an initial iteration for the horizontal velocity, $u^0(x, y)$, vanishing at the upper surface, equal to s at the lower one and satisfying the flux condition

$$\int_0^h u^0(x, y)\, dy = Q. \tag{10}$$

After some easy computations, we can obtain the following expression

$$u^0(x,y) = \left(\frac{s\,h}{2} - Q\right)\,\frac{6}{h^3}\,(y^2 - y\,h) + s\,\left(1 - \frac{y}{h}\right)\,. \tag{11}$$

Next, replacing u by u^0 in (6) we get

$$\frac{d}{d\,x}\left[\left(\frac{h^3}{\mu} - 12\,\alpha\,\int_0^h y(h-y)\,\frac{\partial\,u^0}{\partial\,x}\,dy\right)\,\frac{d\,p^1}{d\,x}\right] = 6\,s\,\frac{d\,h}{d\,x},$$

so that, after an easy integration, the following *first iteration* alternative model for the pressure can be obtained

$$\frac{d}{d\,x}\left[\left(\frac{h^3}{\mu} - 12\,\alpha\,\frac{d\,h}{d\,x}\,\left(\frac{s\,h^2}{30} - \frac{Q\,h}{10}\right)\right)\,\frac{d\,p^1}{d\,x}\right] = 6\,s\,\frac{d\,h}{d\,x}. \tag{12}$$

Now, if expression (11) for $u^0(x,y)$ is introduced in (4) we deduce the following expression for v^0:

$$v^0(x,y) = \left(\frac{2\,s}{h^3} - \frac{6\,Q}{h^4}\right)\,\frac{d\,h}{d\,x}\,y^3 + \left(-\frac{2\,s}{h^2} + \frac{6\,Q}{h^3}\right)\,\frac{d\,h}{d\,x}\,y^2. \tag{13}$$

In order to deduce the model for the next iteration, we start by replacing the previous expression of v^0 in equation (4), and then we use (5) to obtain

$$\begin{aligned} u^1(x,y) \;&=\; s\,\left(1 - \frac{y}{h}\right) + \frac{1}{2\,\mu}\,\frac{d\,p^1}{d\,x}\,(y^2 - y\,h) \\ &\quad +2\,\alpha\,\frac{d\,p^1}{d\,x}\,\left[\int_0^y v^0(x,y)\,dy - \frac{y}{h}\,\int_0^h v^0(x,y)\,dy\right], \end{aligned} \tag{14}$$

or equivalently,

$$\begin{aligned} u^1(x,y) \;&=\; s\,\left(1 - \frac{y}{h}\right) + \frac{1}{2\,\mu}\,\frac{d\,p^1}{d\,x}\,(y^2 - y\,h) \\ +2\,\alpha\,\frac{d\,p^1}{d\,x}\,\frac{d\,h}{d\,x}\,&\left[\left(\frac{s}{2\,h^3} - \frac{3\,Q}{2\,h^4}\right)\,y^4 + \left(-\frac{2\,s}{3\,h^2} + \frac{2\,Q}{h^3}\right)\,y^3 + \left(\frac{s}{6} - \frac{Q}{2\,h}\right)\,y\right]\,. \end{aligned} \tag{15}$$

Next, in (6) we can consider $u = u_1$ to obtain the *second iteration* in the pressure

$$\frac{d}{d\,x}\left[\left(\frac{h^3}{\mu} - 12\,\alpha\,\int_0^h y(h-y)\,\frac{\partial\,u^1}{\partial\,x}\,dy\right)\,\frac{d\,p^2}{d\,x}\right] = 6\,s\,\frac{d\,h}{d\,x}, \tag{16}$$

so that, replacing u_1 by expression (15), we get

$$\frac{d}{d\,x}\left[\left(\frac{h^3}{\mu} - 12\,\alpha\,I_2\right)\,\frac{d\,p^2}{d\,x}\right] = 6\,s\,\frac{d\,h}{d\,x}, \tag{17}$$

where

$$
\begin{aligned}
I_2 = \; & \frac{s\,h^2}{12}\,\frac{d\,h}{d\,x} + \frac{\alpha}{\mu}\left(\frac{d\,p^1}{d\,x}\right)^2 \frac{h^5}{60} - \frac{h^5}{60\,\mu}\frac{d^2\,p^1}{d\,x^2} - \frac{h^4}{24\,\mu}\,\frac{d\,h}{d\,x}\,\frac{d\,p^1}{d\,x} \\
& + \alpha\left(\frac{d^2\,p^1}{d\,x^2}\,\frac{d\,h}{d\,x} + \frac{d\,p^1}{d\,x}\,\frac{d^2\,h}{d\,x^2}\right)\left(\frac{s\,h^4}{140} - \frac{3\,Q\,h^3}{140}\right) \\
& + \alpha\,\frac{d\,p^1}{d\,x}\,\left(\frac{d\,h}{d\,x}\right)^2\left(\frac{11\,s\,h^3}{630} - \frac{13\,Q\,h^2}{420}\right).
\end{aligned}
$$

Next, v^1 can be computed and the continuation of the fixed point iteration procedure allows to subsequently define u^2, p^2 and v^2, and so on. In this way, this fixed point technique provides a family of alternative models. However, it does not seem possible to obtain a generic procedure and the complexity of the involved expressions is increasing; this being the main reason why we just consider in this paper the modified Reynolds equation (12) produced by the *first iteration*. Thus, the alternative Reynolds equation here proposed to model piezoviscous regimes is the following one:

$$
\frac{d}{d\,x}\left[\left(\frac{h^3}{\mu} - 12\,\alpha\,\frac{d\,h}{d\,x}\left(\frac{s\,h^2}{30} - \frac{Q\,h}{10}\right)\right)\frac{d\,p}{d\,x}\right] = 6\,s\,\frac{d\,h}{d\,x}, \tag{18}
$$

where p is the unknown pressure and μ denotes the viscosity that depends on the pressure through Barus law.

Notice that (18) can be understood as a kind of conservation equation for the flow rate

$$
Q = \frac{s\,h}{2} - \frac{h^3}{12\,\mu}\,\frac{d\,p}{d\,x} + \alpha\,\frac{d\,h}{d\,x}\left(\frac{s\,h^2}{30} - \frac{Q\,h}{10}\right)\,\frac{d\,p}{d\,x}\,. \tag{19}
$$

3. Cavitation model and scaling

As indicated in the review paper [5] and throughout the literature, cavitation is one of the most relevant features of lubrication problems. This phenomenon is defined in [10] as the rupture of the continuous fluid film due to the formation of air bubbles inside. The presence of two different regions, the first with a complete fluid film and the second with a partial film (partial lubrication in cavitated area), has been experimentally observed in many lubricated devices such as journal–bearings, ball–bearings, etc.

A review concerning the mathematical and physical analysis of the different models is presented in [3]. The common feature of the models lies in the domain decomposition into two parts: a lubrication region where the appropriate Reynolds equation is verified and a cavitation region where the pressure is taken to be a constant (the vapor saturation pressure). The difference between models comes from the condition imposed on the (unknown) free boundary that separates lubricated and cavitated areas. The two most widely used models are the so called Reynolds (or Swift–Stieber) and Elrod–Adams ones.

The Reynolds model for cavitation starts from the consideration that the pressure in the whole domain is greater than the (known) saturation pressure, thus giving rise to an important number of mathematical papers that use the theory of variational inequalities by associating this model to an obstacle problem. This idea is reinforced by the fact that initially the most popular numerical method used to cope with cavitation in mechanical engineering rely on this approach. Furthermore, this is the usual first approach to cavitation when new Reynolds equations appear. So, in the present paper we propose this model to take into account cavitation and leave the more complex Elrod–Adams model for forthcoming studies.

Reynolds model for cavitation is based on the free boundary condition

$$p = \frac{\partial p}{\partial x} = 0 \tag{20}$$

at the unknown interface between the cavitation and lubrication region.

Then, the cavitation model for lubrication admits the following complementarity problem formulation:

$$\frac{d}{d\,x}\left[\left(\frac{h^3}{\mu} - 12\,\alpha\,\frac{d\,h}{d\,x}\left(\frac{s\,h^2}{30} - \frac{Q\,h}{10}\right)\right)\frac{d\,p}{d\,x}\right] \geq 6\,s\,\frac{d\,h}{d\,x}, \tag{21}$$

$$p \geq 0, \tag{22}$$

$$\left\{\frac{d}{d\,x}\left[\left(\frac{h^3}{\mu} - 12\,\alpha\,\frac{d\,h}{d\,x}\left(\frac{s\,h^2}{30} - \frac{Q\,h}{10}\right)\right)\frac{d\,p}{d\,x}\right] - 6\,s\,\frac{d\,h}{d\,x}\right\}\cdot p = 0. \tag{23}$$

In order to compare the results with those ones appearing in [15] for the case of a *rigid long rolling–cylinder*, we introduce the angular coordinate, t, defined by the change of variable

$$x = R\,\sin(t),\ t \in [-\pi/2, \pi/2],$$

where R represents the radius of the cylinder. Then, we define the film thickness by

$$h(t) = -\frac{R}{n}(1 + n\,\cos(t)), \quad n = -\frac{R}{h_0 + R}, \quad h_0 = h(0)\,,$$

where h_0 is the minimum of the thickness. Moreover, we introduce the following scaled magnitudes:

$$\overline{h} = -\frac{n\,h}{R},\ \ \overline{\mu} = \frac{\mu}{\mu_0},\ \ \overline{p} = \frac{p\,h_0}{\mu_0\,s},\ \ \overline{\alpha} = \frac{\alpha\,\mu_0\,s}{h_0},\ \ \overline{\beta} = \overline{\alpha}\frac{h_0}{R}.$$

and the scaled flow rate

$$\overline{Q} = -\frac{n\,Q}{sR} \ = \ \frac{\overline{h}}{2} + \left[\frac{\overline{h}^3\ \mathrm{e}^{-\overline{\alpha p}}}{12\,n\,\overline{h}_0\,\cos(t)} + \frac{\overline{\beta}\,\sin(t)}{\overline{h}_0\,\cos^2(t)}\left(\frac{\overline{h}^2}{30} - \frac{\overline{Q}\,\overline{h}}{10}\right)\right]\,\frac{d\,\overline{p}}{d\,t}\,. \tag{24}$$

Once we consider this scaling in the previously described Reynolds model for cavitation, then $\overline{p}$ can be obtained as the solution of the following dimensionless

complementarity problem posed in the domain $\Omega = (-\pi/2, \pi/2)$):

$$\frac{d}{d\,t}\left(G(t,\overline{p})\,\frac{d\,\overline{p}}{d\,t}\right) \geq 6\,\frac{d\,\overline{h}}{d\,t} \qquad \text{in } \Omega, \tag{25}$$

$$\overline{p} \geq 0 \qquad \text{in } \Omega, \tag{26}$$

$$\left[\frac{d}{d\,t}\left(G(t,\overline{p})\,\frac{d\,\overline{p}}{d\,t}\right) - 6\,\frac{d\,\overline{h}}{d\,t}\right]\overline{p} = 0 \qquad \text{in } \Omega, \tag{27}$$

jointly with the boundary conditions $\overline{p}(-\pi/2) = 0$, $\overline{p}(\pi/2) = 0$. The term G is defined by

$$G(t,\overline{p}) = \left(\overline{h}^3\ \mathrm{e}^{-\overline{\alpha p}} - \frac{12\,\overline{\beta}}{\cos(t)}\,\frac{d\,\overline{h}}{d\,t}\left(\frac{\overline{h}^2}{30} - \frac{\overline{Q}\,\overline{h}}{10}\right)\right)\,\frac{1}{-n\,\overline{h}_0\,\cos(t)}\,, \tag{28}$$

where $\overline{h}_0$ denotes the minimum of the dimensionless gap.

On the other hand, if we introduce the unknown lubrication and cavitation regions

$$\Omega^+ = \{t \in \Omega / \overline{p}(t) > 0\}, \quad \Omega_0 = \{t \in \Omega / \overline{p}(t) = 0\},$$

then the following equations hold:

$$\frac{d}{d\,t}\left(G(t,\overline{p})\,\frac{d\,\overline{p}}{d\,t}\right) = 6\,\frac{d\,\overline{h}}{d\,t}\,, \ \ \overline{p} > 0 \qquad \text{in } \Omega^+, \tag{29}$$

$$\overline{p} = 0 \qquad \text{in } \Omega_0, \tag{30}$$

$$\overline{p}(t_2) = \frac{d\,\overline{p}}{d\,t}(t_2) = 0. \tag{31}$$

Notice that the so called smooth pasting condition (31) at the free boundary actually corresponds to the conservation of the scaled flow rate (24) through the unknown interface, t_2, separating the lubrication and cavitation regions. By using (24) and (31) we can rewrite G in the form

$$G(t,\overline{p}) = \left(\overline{h}^3\ \mathrm{e}^{-\overline{\alpha p}} - \frac{12\,\overline{\beta}}{\cos(t)}\,\frac{d\,\overline{h}}{d\,t}\left(\frac{\overline{h}^2}{30} - \frac{\overline{h}\,\overline{h}_2}{20}\right)\right)\,\frac{1}{-n\,\overline{h}_0\,\cos(t)}\,, \tag{32}$$

where $\overline{h}_2 = \overline{h}(t_2)$ at the unknown free boundary t_2.

It is important to point out that the model (25)-(27), or the equivalent set of equations (29)-(31), includes the isoviscous case for $\overline{\alpha} = \overline{\beta} = 0$ and the classical piezoviscous model for the choice $\overline{\alpha} \neq 0$ and $\overline{\beta} = 0$. Furthermore, the Rajagopal & Szeri model in [15] may be also written in a similar way, although with the following slightly different expression of G:

$$G(t,\overline{p}) = \left(\overline{h}^3\ \mathrm{e}^{-\overline{\alpha p}} + \frac{\overline{\beta}\,\overline{h}_2}{2\,\cos(t)}\,\frac{d\,\overline{h}^2}{d\,t}\right)\,\frac{1}{-n\,\overline{h}_0\,\cos(t)}\,. \tag{33}$$

4. An alternative first order model

Following some ideas in [15], another alternative is to restart from the modified Reynolds equation (18), to integrate it and interpret the result as a kind of conservation equation for the flow rate Q given by (19).

Therefore, from (19) we can pose the following first order ordinary differential equation:

$$\frac{d\,p}{d\,x} = \frac{\dfrac{s\,h}{2} - Q}{\dfrac{h^3}{12\,\mu} - \alpha\,\dfrac{d\,h}{d\,x}\left(\dfrac{s\,h^2}{30} - \dfrac{Q\,h}{10}\right)} \,. \tag{34}$$

So, by introducing the change of variable $x = R\,\sin(t)$, rescaling as before and taking into account the expression (24) and the condition (31), the next dimensionless initial value ode problem is obtained:

$$\frac{d\,\overline{p}}{d\,t} = \frac{6\,(-n)\,\overline{h}_0\,\cos^2(t)\,\left[\overline{h} - \overline{h}_2\right]}{\overline{h}^{\,3}\,\mathrm{e}^{-\overline{\alpha p}}\,\cos(t) + \dfrac{6}{5}\,\overline{\beta}\,n\,\sin(t)\,\overline{h}\left[\dfrac{\overline{h}}{3} - \dfrac{\overline{h}_2}{2}\right]} \tag{35}$$

$$\overline{p}(-\pi/2) = 0 \,. \tag{36}$$

It is important to notice that the solution of (35)-(36) satisfying $\overline{p}(t_2) = 0$ is the solution of (29)-(31).

Analogously, the corresponding *first order ODE version* for isoviscous, classical piezoviscous and Rajagopal & Szeri models can be obtained.

5. Numerical methods

Two different formulations have been posed for the alternative piezoviscous model which can also be applied to the other piezoviscous and isoviscous models. In this section, several numerical schemes are proposed to obtain the numerical solutions of these problems involving first order ODE solvers, finite elements method, projected relaxation algorithms and duality type method.

5.1. Numerical solution of the alternative Reynolds equation

The numerical solutions for the problem (25)-(27) may be obtained by the combination of finite element techniques with a classical projection method [9] or a more complex duality type algorithm proposed in [6]. The application of these techniques to classical piezoviscous formulations can be found in [12, 4, 13, 7], for example. The departure point is the formulation of the complementarity problem in terms of an equivalent variational inequality formulation. More precisely, the solution of problem (25)-(27) jointly with the boundary conditions satisfies that $\overline{p} \in K$ and

$$\int_{-\pi/2}^{\pi/2} G(t,\overline{p})\,\overline{p}'\,(\varphi - \overline{p})'\,dt \geq -6\int_{-\pi/2}^{\pi/2} \overline{h}'\,(\varphi - \overline{p})dt, \quad \forall \varphi \in K, \tag{37}$$

where

$$K = \{\varphi \in H_0^1(\Omega)/\varphi \geq 0\}$$

and $H_0^1(\Omega)$ denotes the classical Sobolev space.

Starting from $\overline{p}^0$, solution of the isoviscous case, we apply a fixed point algorithm for the nonlinearity related to piezoviscosity. At $(n+1)$-th iteration, for a given $\overline{p}^n$, we obtain $\overline{p}^{n+1} \in K$, such that

$$\int_{-\pi/2}^{\pi/2} G(t,\overline{p}^n)\,(\overline{p}^{n+1})'\,(\varphi - \overline{p}^{n+1})'\,dt \geq -6\int_{-\pi/2}^{\pi/2} \overline{h}'\,(\varphi - \overline{p}^{n+1})dt, \quad \forall \varphi \in K,$$

with $G(t,\overline{p})$ given by expression (32) for the alternative model here proposed and by (33) for the Rajagopal & Szeri one.

For the spatial discretization we consider a classical piecewise linear Lagrange finite element space, so that the discretized problem consists of finding $\overline{p}_h^{n+1} \in K_h$, such that

$$\int_{-\pi/2}^{\pi/2} G(t,\overline{p}_h^n)\,(\overline{p}_h^{n+1})'\,(\varphi_h - \overline{p}_h^{n+1})'\,dt \geq -6\int_{-\pi/2}^{\pi/2} \overline{h}'\,(\varphi_h - \overline{p}_h^{n+1})dt,\ \forall \varphi_h \in K_h, \tag{38}$$

where V_h denotes the finite element space (see [8], for example):

$$V_h = \{\varphi_h \in C^0(\Omega)\,/\varphi_h|_E \in P_1,\ \forall E \in \tau_h\},$$

E being a standard element of the finite element mesh, the subspace V_{0h} is given by

$$V_{0h} = \{\varphi_h \in V_h\,/\varphi_h(-\pi/2) = 0,\ \varphi_h(\pi/2) = 0\},$$

and the convex set K_h is defined by

$$K_h = \{\varphi_\in V_{0h}\,/\varphi_h(x_i) \geq 0,\ \forall i \text{ node of } \tau_h\}.$$

For simplicity, hereafter we omit the natural dependence h in the unknown $\overline{p}$ and the functions in the finite element space, h being the stepsize of the uniform finite element mesh.

At this point we propose two alternatives to solve the discretized problem (38): a relaxation algorithm with projection on the convex set K_h first described in [9] and the duality type algorithm proposed in [6] for the numerical solution partial differential equations involving maximal monotone operators. As the first one is classical we describe the application of the second one.

In order to apply the duality method in [6], we introduce the indicatrix function of the convex K_h denoted by I_{K_h}, so that the variational inequality of first kind (38) can be transformed in the equivalent variational inequality of second kind that consists of finding $\overline{p}^{n+1} \in V_{0h}$, such that

$$\int_{-\pi/2}^{\pi/2} G(t,\overline{p}^n)\,(\overline{p}^{n+1})'\,(\varphi - \overline{p}^{n+1})'\,dt + I_{K_h}(\varphi) - I_{K_h}(\overline{p}^{n+1}) \quad \geq$$

$$-6\int_{-\pi/2}^{\pi/2} \overline{h}'\,(\varphi - \overline{p}^{n+1})dt, \qquad \forall \varphi \in V_{0h}.$$

Moreover, we use the notation

$$\begin{aligned}(A^n\,\overline{p}^{n+1},\varphi) &= \int_{-\pi/2}^{\pi/2} G(t,\overline{p}^n)\,(\overline{p}^{n+1})'\,(\varphi-\overline{p}^{n+1})'\,dt,\\ (f^n,\varphi) &= -6\int_{-\pi/2}^{\pi/2}\overline{h}'\,(\varphi-\overline{p}^{n+1})\,dt.\end{aligned}$$

Then, using the tools of subdifferential calculus, we obtain that

$$\gamma^{n+1} = -(A^n\,\overline{p}^{n+1} - f^n) \in \partial\, I_K(\overline{p}^{n+1}), \tag{39}$$

where $\partial\, I_{K_h}$ denotes the subdifferential of the indicatrix function. Therefore, the variational inequality problem defined by (39) is equivalent to the problem:

Find $\overline{p}^{n+1} \in V_{0h}$, such that

$$\begin{aligned}\int_{-\pi/2}^{\pi/2} G(t,\overline{p}^n)\,(\overline{p}^{n+1})'\,\varphi'\,dt + \int_{-\pi/2}^{\pi/2}\gamma^{n+1}\,\varphi\,dt &= \\ -6\int_{-\pi/2}^{\pi/2}\overline{h}'\,\varphi\,dt, \qquad \forall\varphi\in V_{0h}, &\qquad (40)\\ \gamma^{n+1}\in\partial\, I_K(\overline{p}^{n+1}). &\qquad (41)\end{aligned}$$

As the multivalued operator $\partial\, I_{K_h}$ is the subdiferencial of indicatrix function I_{K_h} then it is a maximal monotone. In order to apply the results in [6], for a given parameter $\omega > 0$, we introduce the new variable

$$\beta^{n+1} \in \partial\, I_{K_h}(\overline{p}^{n+1}) - \omega\,\overline{p}^{n+1}. \tag{42}$$

In terms of this new variable β^{n+1}, the equivalent formulation to (40)-(41) can be written in the form:

Find $\overline{p}^{n+1} \in V_{0h}$, such that

$$\int_{-\pi/2}^{\pi/2} G(t,\overline{p}^n)\,(\overline{p}^{n+1})'\,\varphi'\,dt + \int_{-\pi/2}^{\pi/2}(\beta^{n+1}+\omega\,\overline{p}^{n+1})\,\varphi\,dx =$$

$$-6\,s\int_{-\pi/2}^{\pi/2}\overline{h}'\,\varphi\,dt, \quad \forall\varphi\in V_{0h}, \tag{43}$$

$$\beta^{n+1}\in\partial\, I_K(\overline{p}^{n+1}) - \omega\,\overline{p}^{n+1}, \tag{44}$$

with $\omega > 0$.

Then by using a lemma appearing in [6], we have that (44) is equivalent to

$$\beta^{n+1} = K_\lambda^\omega(\overline{p}^{n+1} + \lambda\,\beta^{n+1}), \tag{45}$$

where K_λ^ω denotes the Yosida approximation of the operator $\partial I_{K_h} - \omega I$ with parameter $\lambda > 0$, we drop the dependence on h for the operator K_λ^ω.

Next, we summarize the steps of duality algorithm to solve (43)-(44) as follows:

- Initialize β_0^{n+1}.
- At step $j+1$, for a given β_j^{n+1}, obtain $\overline{p}_{j+1}^{n+1}$ as the solution of the following linear problem:

$$\int_{-\pi/2}^{\pi/2} G(t,\overline{p}^n)\ (\overline{p}_{j+1}^{n+1})'\ \varphi'\,dt + \omega \int_{-\pi/2}^{\pi/2} \overline{p}_{j+1}^{n+1}\,\varphi\,dx =$$

$$-\int_{-\pi/2}^{\pi/2} \beta_j^{n+1}\,\varphi\,dx - 6\int_{-\pi/2}^{\pi/2} \overline{h}'\ \varphi\,dt, \quad \forall \varphi \in V_{0h}, \tag{46}$$

- Update the value of β_{j+1}^{n+1} with

$$\beta_{j+1}^{n+1} = K_\lambda^\omega(\overline{p}_j^{n+1} + \lambda\,\beta_j^{n+1}), \tag{47}$$

- Repeat the previous two steps until satisfying of the convergence test in sequence $\{\overline{p}_j^{n+1}\}$ in index j.

We note that the analytical expression of K_λ^ω allows to update in (47) with

$$\beta_{j+1}^{n+1} = \frac{(\overline{p}_j^{n+1} + \lambda\,\beta_j^{n+1}) - P_{K_h}(\overline{p}_j^{n+1} + \lambda\,\beta_j^{n+1})}{\lambda(1-\lambda\,\omega)} - \omega\,(\overline{p}_j^{n+1} + \lambda\,\beta_j^{n+1}), \tag{48}$$

where P_{K_h} denotes the projection operator onto the convex K_h. Some convergence results have been proved in [6] under the constraint $\lambda\,\omega \leq 1/2$, so that here we take $\lambda\,\omega = 1/2$ in all tests.

5.2. Numerical solution of the first order ODE problem

In the numerical solution of the first order ODE problem we have to compute the pressure $\overline{p}$ that satisfies the initial value problem (35)-(36) and the point t_2 such that $\overline{p}(t_2) = 0$ and $\overline{p}'(t_2) = 0$.

For this purpose, the proposed iterative numerical scheme combines a *regula falsi* algorithm that builds a sequence $\{t_2^k\}$ in the interval $(0, \pi/2)$, designed to converge to t_2, with the use of the `ode15s` integrator of MATLAB to solve the initial value problem in $[-\pi/2, t_2^k]$, for each value of t_2^k. So, the sketch of the algorithm is as follows:

- Start *regula falsi* with the interval $[t_2^0, t_2^1] = [0, \pi/2]$.

- At the step k, for a given t_2^k , solve the initial value problem

$$\frac{d\,\overline{p}^k}{d\,t} = \frac{-6n\,\cos(t)(\overline{h}-\overline{h}_2^k)\,\overline{h}_0}{\overline{h}^3\;\mathrm{e}^{-\overline{\alpha}\,\overline{p}} + \dfrac{6}{5}\overline{\beta}\,n\,\tan(t)\,\overline{h}\left[\dfrac{\overline{h}}{3}-\dfrac{\overline{h}_2^k}{2}\right]} \quad \text{in } (-\pi/2, t_2^k]$$

$$\overline{p}^k(-\tfrac{\pi}{2}) = 0$$

  where $\overline{h}_2^k = \overline{h}(t_2^k)$

- if $\overline{p}^k(t_2^k) \neq 0$, update t_2^{k+1} using *regula falsi*

After convergence, the final solution is extended to the interval $[-\pi/2, \pi/2]$ by $\overline{p}^k(t) = 0$ in $(t_2^k, \pi/2]$.

6. Numerical tests

In order to assess the relevance of the extra terms of both new more rigorous models for the piezoviscous case when compared with the classical piezoviscous formulation, several numerical tests have been carried out. The idea is to make a comparative analysis of the different models, formulations and numerical schemes presented in the previous sections, mainly taking as a reference the data set of the numerical examples in [15]. Although in the presence of high pressures the cylinder will deformed, in the present paper to illustrate the differences we restrict ourselves to the case of a rigid cylinder. In a future work, the elastohydrodynamic case will be treated. So, these data are $\overline{\alpha} = 9.293 \times 10^{-3}$ and $\overline{\beta} = \overline{\alpha}/ratio$, with $ratio = 10^4$. In addition, the value $ratio = 10^3$, is introduced here to analyze a less extreme case. We recall again that to reproduce the classical piezoviscous model $\overline{\beta} = 0$ can be chosen and for the isoviscous case $\overline{\alpha} = \overline{\beta} = 0$ can be considered.

For the solution of the variational inequality model with the projected relaxation numerical scheme, labeled by [VI-Rel-R] in the forthcoming tables and figures, in all tests a uniform finite element mesh with 80000 nodes on the interval $[-\pi/2, \pi/2]$ has been chosen and a relaxation parameter equal to 1.99 has been considered. Moreover, for the inner relaxation algorithm and for the outer fixed point iteration method, the tolerances for the stopping tests have been taken equal to 10^{-12} and 5×10^{-6}, respectively.

For the solution of the variational inequality model with the duality method, labeled by [VI-BM-R], the same discretization is taken on the interval $[-\pi/2, \pi/2]$. In addition, for $ratio = 10^3$ the chosen parameters are $\omega = 0.9$ and a tolerance of 10^{-6} in the duality algorithm stopping test, while for $ratio = 10^4$ this parameters are $\omega = 0.07$ and a tolerance of 5×10^{-7}. For both cases a tolerance of 10^{-3} for the fixed point stopping test is chosen.

In the numerical scheme implemented for the first order ODE formulation, labeled by [ODE-R], a 40000 nodes discretization of each interval $[-\frac{\pi}{2}, t_2^k]$ is

taken, thus leading to a similar stepsize to the one used in the meshes for the previous methods. Furthermore, the MATLAB `ode15s` integration function, with `RelTol`= 10^{-6} and `AbsTol`= 10^{-5}, is combined with a *regula falsi* algorithm with a stopping test of 5×10^{-5}.

Table 1 shows the computed maximum of the dimensionless pressure with the different models, formulations and numerical schemes for the less extreme case with $ratio = 10^3$ and Table 2 shows the corresponding computed free boundary point t_2. For the isoviscous case, the exact results provided by an analytical solution are included as a reference.

Table 1: Maximum values of $\overline{p}$ for the different models, formulations and numerical schemes with $ratio = 10^3$

	ODE-R	VI-BM-R	VI-Rel-R	Analytical
Isoviscous	33.9235	33.9098	33.9129	33.9229
Piezo classical	40.7514	40.7324	40.7340	
Piezo Szeri	40.7562	40.7370	40.7387	—
Piezo Alternative	40.7508	40.7332	40.7347	

Table 2: Values of t_2 for the different models, formulations and numerical schemes with $ratio = 10^3$

	ODE-R	VI-BM-R	VI-Rel-R	Analytical
Isoviscous	0.021230	0.019792	0.021237	0.021230
Piezo classical	0.021230	0.019792	0.021237	
Piezo Szeri	0.021230	0.019792	0.021237	—
Piezo Alternative	0.021230	0.019792	0.021237	

Figures 1 and 2 show the dimensionless pressure profile obtained with the diferent numerical schemes for one of the piezoviscous models for the case $ratio = 10^3$; for the other models the behaviour is analogous. So, in this case, the three numerical schemes reach similar solutions and have a similar performance.

Figure 3 shows the maximum values of the dimensionless pressure obtained with the [ODE-R] numerical scheme for all the models in the case with $ratio = 10^3$ and Figure 4 shows the corresponding results for the dimensionless viscosity; for the other numerical schemes the profiles are analogous. In this case, there is almost no difference between the three piezoviscous models.

Table 3 shows the maximum of the dimensionless pressure obtained with the different models, formulations and numerical schemes for the more extreme case with $ratio = 10^4$ and Table 4 shows the free boundary point t_2. For the isoviscous case, the analytical solution values are again included as a reference.

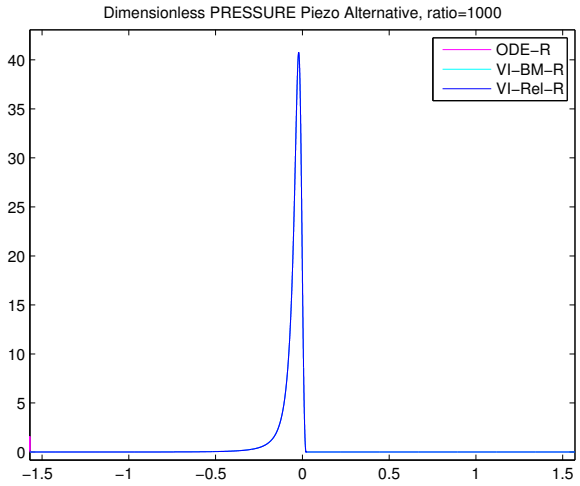

Figure 1: Dimensionless pressure for the three numerical schemes with $ratio = 10^3$ and the proposed alternative piezoviscous model

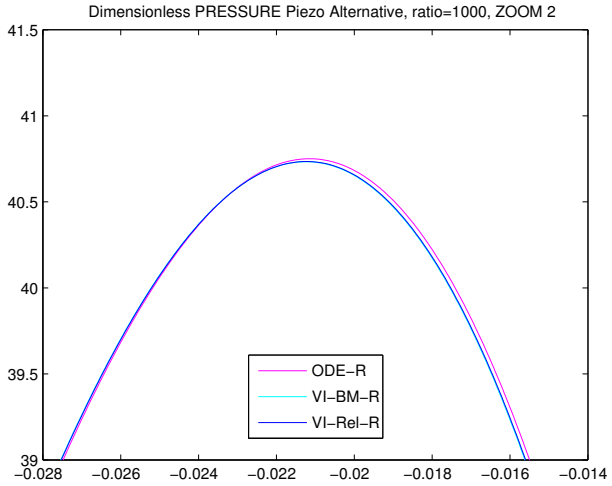

Figure 2: Zoom of the dimensionless pressure maximum for the three numerical schemes with $ratio = 10^3$ and the proposed alternative piezoviscous model

It seems that the results obtained with the numerical schemes here implemented for the Rajagopal & Szeri model are very similar to the solution presented in

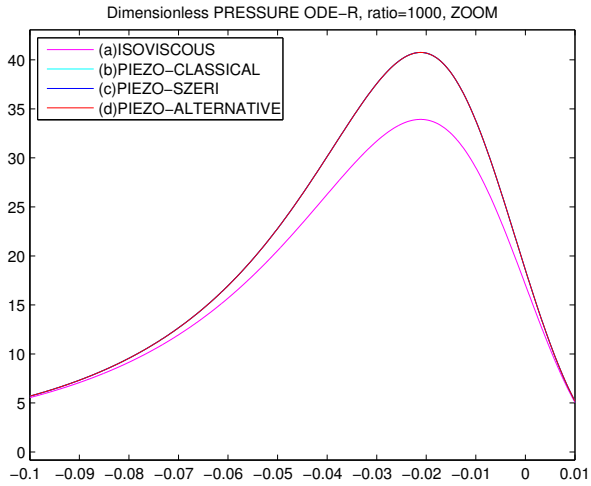

Figure 3: Zoom of the dimensionless pressure maximum for the three piezoviscous models and the isoviscous one with $ratio = 10^3$ and the [ODE-R] numerical scheme

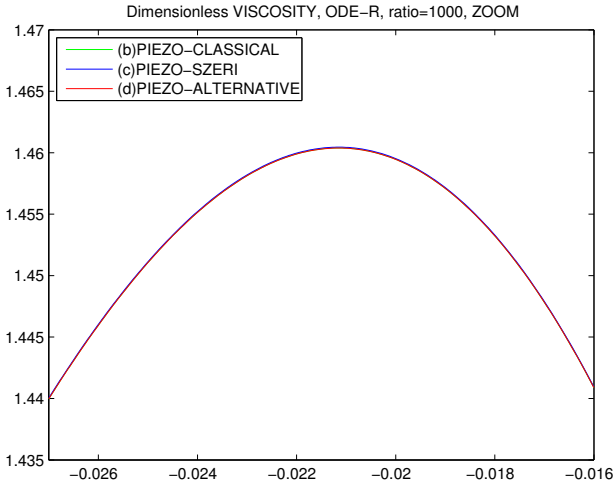

Figure 4: Zoom of the dimensionless viscosity maximum for the three piezoviscous models with $ratio = 10^3$ and the [ODE-R] numerical scheme

[15]. All of them may be used to make a comparison with the solutions of the

other models, but the [ODE-R] scheme seems to provide the closest solutions.

Table 3: Maximum values of $\overline{p}$ for the different models, formulations and numerical schemes with $ratio = 10^4$

	ODE-R	VI-BM-R	VI-Rel-R	Analytical
Isoviscous	107.520	107.582	107.518	107.520
Piezo–Classical	765.787	764.846	759.558	—
Piezo–Szeri	824.881	816.125	812.327	
Piezo–Alternative	771.111	763.493	754.963	

Table 4: Values of t_2 for the different models, formulations and numerical schemes with $ratio = 10^4$

	ODE-R	VI-BM-R	VI-Rel-R	Analytical
Isoviscous	6.7188×10^{-3}	6.2831×10^{-3}	6.7151×10^{-3}	6.7187×10^{-3}
Piezo classical	6.7189×10^{-3}	6.2204×10^{-3}	6.7151×10^{-3}	—
Piezo Szeri	6.7190×10^{-3}	6.2204×10^{-3}	6.7151×10^{-3}	
Piezo Altern.	6.7188×10^{-3}	6.2204×10^{-3}	6.7151×10^{-3}	

Figure 5 shows the dimensionless pressure profile obtained with the different numerical schemes for the here proposed piezoviscous model in the case with $ratio = 10^4$. A slight difference can be observed between the maximum of pressure obtained with the three numerical schemes but all of them have a similar performance.

Figure 6 shows the maximum values of the dimensionless pressure obtained with the [ODE-R] numerical scheme for all the models in the case with $ratio = 10^4$. Figure 7 shows the corresponding dimensionless viscosity for these models. In this case, there is a slight difference between the maximum of pressure obtained with the classical piezoviscous model and the here proposed one, while the other model reaches a higher value. For the viscosity, the difference between the maximum value for the Rajagopal & Szeri model and the other two models is greater.

7. Conclusions

In this paper, a rigorous methodology to include piezoviscosity previously to the limit procedures to obtain a Reynolds model has been developed, overcoming a simplification hypothesis considered in [15]. Additionally, by means of a suitable complementarity formulation, the possible presence of cavitation is included.

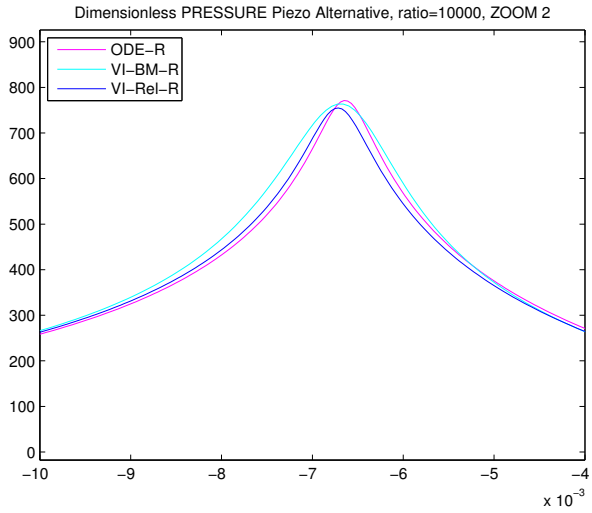

Figure 5: Dimensionless pressure for the three numerical schemes with $ratio = 10^4$ and the proposed alternative piezoviscous model

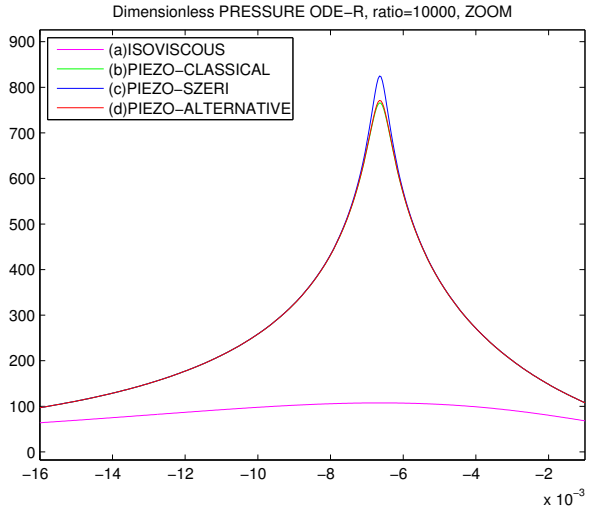

Figure 6: Zoom of the dimensionless pressure maximum for the three numerical schemes with $ratio = 10^4$ and the proposed alternative piezoviscous model

In order to compare the different piezoviscous lubrication models, appropriate numerical techniques are proposed for the variational inequality formulation

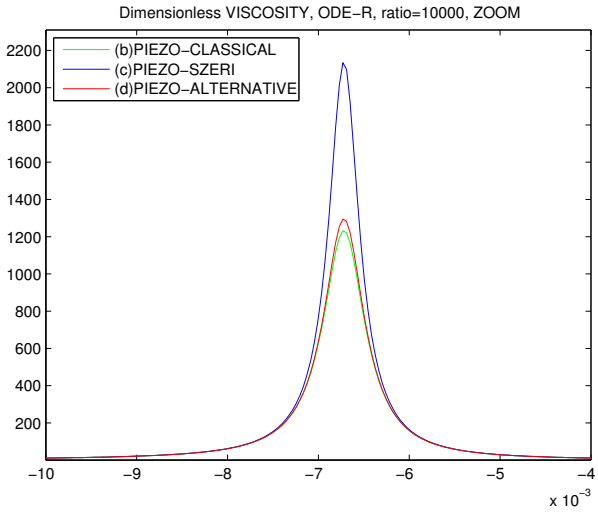

Figure 7: Zoom of the dimensionless viscosity maximum for the three piezoviscous models with $ratio = 10^4$ and the [ODE-R] numerical scheme

for the alternative Reynolds cavitation model and for the first order equation in the lubricated region.

Concerning the numerical results, a first general conclusion is that for critical values of the parameters the pressure exhibits a large gradient near the maximum pressure region, so that it results difficult to capture the *almost spike* qualitative behavior of the solution in all models. Furthermore, in the extreme regime that we have considered, it seems that the numerical results obtained for this new model result to be closer to the ones of the classical model mainly used in mechanical and mathematical literature.

Now, the authors are trying to extend the alternative model when Elrod–Adams model for cavitation is used, as it results more realistic when cavitation regions appear in the convergent region (*starvation phenomenon*). Other forthcoming studies are devoted to the consideration of the elastohydrodynamic lubrication regime.

References

[1] S. Bair, M. Khorsari and W.O. Winner, *High pressure rheology of lubricants and limitation of the Reynolds equation*, Tribol. Int. **10** (1998) 573–586.

[2] G. Bayada and M. Chambat, *The transition between Stokes equations and the Reynolds equation: a mathematical proof*, Appl. Math. Optim. **14(1)** (1986) 73–93.

[3] G. Bayada and M. Chambat, *Sur quelques modélisations de la zone de cavitation en lubrification hydrodynamique*, J. of Theor. and Appl. Mech. **5(5)** (1986) 703–729.

[4] G. Bayada M. El Alaoui and C. Vázquez, *Existence for elastohydrodynamic lubrication problems with a new model for cavitation*, Bol. Soc. Esp. Mat. Apl. **39** (2007) 31–74.

[5] G. Bayada and C. Vázquez, *Existence for elastohydrodynamic lubrication problems with a new model for cavitation*, Euro. Jnal. Appl. Math. **7** (1996) 63–73.

[6] A. Bermúdez and C. Moreno, *Duality methods for solving variational inequalities*, Comp. Math. with Appl. **7** (1981) 43–58.

[7] N. Calvo, J. Durany and C. Vázquez, *Comparación de algoritmos numéricos en problemas de lubricación hidrodinámica con cavitación en dimensión uno*, Rev. Int. Met. Num. Calc. Dis. Ing. **13** (1997) 185–209.

[8] P. Ciarlet, *The Finite Element Method for Elliptic Problems*, North Holland, 1978.

[9] C.W. Cryer, *The solution of a quadratic programming problem using systematic overrelaxation*, SIAM J. Control, **9** (1971) 385–392.

[10] J. Dowson, C.M. Taylor, *Cavitation in bearings*, Ann. Rev. Fluid Mech. (1979) 35–66.

[11] J. Durany, G. García and C. Vázquez, *A mixed Dirichlet–Neumann problem for a nonlinear Reynods equation on elastohydrodynamic lubrication*, Proceedings of the Edinburgh Mathematical Society **39** (1996) 151–162.

[12] J. Durany, G. García and C. Vázquez, *Numerical computation of free boundary problems in elastohydrodynamic lubrication*, Appl. Math. Modelling **20** (1996) 104–113.

[13] J. Durany, G. García and C. Vázquez, *An elastohydrodynamic coupled problem between a piezoviscous equation and a hinged plate model*, Mathematical Modelling and Numerical Analysis **31** (1997) 495–516.

[14] J.A. Greenwood, *Thining Films and Tribology Interfaces*, Proceedings of 26th Leeds–Lyon Symp. (ed. D. Dowson), Tribology Series , **28** (2000) 703–794.

[15] K. R. Rajagopal and A. Z. Szeri, *On an inconsistency in the derivation of the equations of elastohydrodynamic lubrication*, Proc. R. Soc. Lond. **A 459** (2003) 2771–2786.

[16] O. Reynolds, *On the theory of lubrication and its application to the Tower's experiments*, Phil Trans. R. Soc. Lond. **177** (1886) 159–209.

[17] C.T. Schafer, P. Giese, W.P. Rowe, N.H. Woolley, *Elastohydrodynamically lubricated line contact based on the Navier–Stokes equations*, in Thining Films and Tribology Interfaces, Proceedings of 26th Leeds–Lyon Symp. (ed. D. Dowson), Tribology Series , **28** (2000) 57–68.

[18] A. Z. Szeri, *Fluid film lubrication: theory and design*, Cambridge University Press, 1998.

[19] C. Vázquez, *Existence and uniqueness of solution for a lubrication problem in a journal bearing with axial supply*, Advances in Mathematical Science and Applications **4** (1994) 313–331.